

Photochemical & Photobiological Sciences

Accepted Manuscript



This is an *Accepted Manuscript*, which has been through the Royal Society of Chemistry peer review process and has been accepted for publication.

Accepted Manuscripts are published online shortly after acceptance, before technical editing, formatting and proof reading. Using this free service, authors can make their results available to the community, in citable form, before we publish the edited article. We will replace this *Accepted Manuscript* with the edited and formatted *Advance Article* as soon as it is available.

You can find more information about *Accepted Manuscripts* in the [Information for Authors](#).

Please note that technical editing may introduce minor changes to the text and/or graphics, which may alter content. The journal's standard [Terms & Conditions](#) and the [Ethical guidelines](#) still apply. In no event shall the Royal Society of Chemistry be held responsible for any errors or omissions in this *Accepted Manuscript* or any consequences arising from the use of any information it contains.

Cite this: DOI: 10.1039/c0xx00000x

www.rsc.org/xxxxxx

ARTICLE TYPE

“Turn-On” fluorescent chemosensor for Zinc (II) dipodal ratiometric receptor: Application in live cell imaging.

Kundan Tayade^{a,b}, Banashree Bondhopadhyay^d, Hemant Sharma^c, Anupam Basu^d, Vikas Gite^a, Sanjay Attarde^b, Narinder Singh^{*c}, Anil Kuwar^{*a}

Received (in XXX, XXX) Xth XXXXXXXXX 20XX, Accepted Xth XXXXXXXXX 20XX

DOI: 10.1039/b000000x

A dipodal ligand 2,2'-((ethane-1,2-diylbis(azanediy))bis(ethane-1,1-diyl)diphenol was synthesized through condensation reaction and was characterized with IR, ¹H NMR, ¹³C-NMR, and mass spectroscopy. The receptor **2** has shown marked enhancement in fluorescence intensity (emission signal at 341 nm) on binding with the Zn²⁺ compared to other surveyed metal ions. The sensor has shown dramatic changes in dual channel fluorescence emission with λ_{max} at 300 and 341 nm. The successive addition of Zn²⁺ to the solution of sensor lead to blue shift the peak maxima and interestingly upon addition of higher equivalents of Zn²⁺ quenches the fluorescence intensity of sensor and ultimately original fluorescent profile of sensor is restored. The structures of **2** and **3** were optimized with B3LYP/LanL2DZ basis sets. The receptor **2** was successfully detect the Zn²⁺ ion in HeLa cells cultured in Zn²⁺ enriched medium.

15 Introduction

The research arena of supramolecular chemistry is appending towards the synthesis of simple, cost effective noncyclic receptors; which avails the distinct fluorescence-based detection of physiologically important metal ions.¹⁻⁵ Several metal ions play a crucial role in physiological processes as long as they do not exceed the cellular needs.⁶⁻⁹ Zn²⁺ has an indispensable role in many biological processes such as Zn²⁺ is involved in stimulation of more than 100 enzymes in the body.¹⁰⁻¹³ Now a day the role of Zn²⁺ in neurobiology was thoroughly explored; such as, neuronal passing can occur as a result of abandoned Zn²⁺ ion released after stressful brain injury, stroke, or seizure.¹⁴⁻¹⁶ Zn²⁺ also stimulate the production of α-amyloid leading to Alzheimer's disease and other neurological threats.¹⁷ Moreover, the excess of Zn²⁺ present in the soil may lead to suspend the activities of several important microbes. The regulated amounts of Zn²⁺ is important for the physiological functioning of flora and fauna;¹⁸ thus Zn²⁺ is often considered as an interesting paradox to life and highlight the importance of detection methods for Zn²⁺ recognition in environmental and biological samples.

The deficiency of proper detecting probe for over a quite large concentration range and exhibiting high binding affinity causes a severe interference for further surveys of this metal ion.¹⁹ Most of the reported sensors for Zn²⁺ ion shows deprived binding affinity towards Zn²⁺ ion and suffer strong interference effects.^{20,21} A significant effort has been dedicated to the improvement of Zn²⁺ selective fluorescent receptors in the last decade. However, in most cases fluorescence changes can only be observed in non-aqueous solvent and as well as affected by the common interference of other cations, which bound the limits for their analytical application in environmental real samples. Therefore,

the development of highly sensitive and selective fluorescent receptor for Zn²⁺ ion in aqueous solution is very important and is still stimulating task for the researchers.²²

Herein, we explored the new application of receptor **2** as cation sensor with “Turn-ON” mechanism based upon the concentration of metal ion. It is merit to mention that, compared to the previously reported receptors for Zn²⁺ our synthesized receptor shown a comparable affinity towards zinc ion with low detection limit.²³⁻²⁷

55 Experimental

General Information

IR spectra were recorded on a Perkin Elmer Spectrum one spectrometer, using Nujol Mull. ¹H and ¹³C NMR spectra were obtained on a Bruker AVANCE DMX400 spectrometer in DMSO-d₆ as solvent. Fluorescence measurements were made with a HORIBA JOBIN YVON, Fluoromax-4 Spectrofluorometer. UV-Vis absorption spectra were recorded on Shimadzu UV-2450 spectrophotometer. The fluorescence images were recorded on Leica DM 1000 fluorescence microscope using UV filter (Excitation-UV, Band Pass range: 340-380 nm, Dichromatic Mirror: 400 nm) and Green Filter (Excitation – Green, Band Pass range: 515-560 nm, Dichromatic Mirror: 580 nm). Thermal analysis study was carried out on Perkin Elmer DSC 400 and Perkin Elmer TGA 400. The solvents were distilled before use to ensure purity. Commercially available reagents were used without further purification.

Synthesis of receptor **2**

Compound **1** was synthesized by refluxing one mole of ethane-1,2-diamine (0.60 g, 10 mmol) with two equivalents of 2-hydroxy acetophenone (2.72 g, 20 mmol) in ethanol (50 ml). Compound **1** was obtained with good yield and appears as a yellow crystalline powder with 70 % yield, mp >250 °C. Further receptor **2** was

obtained from compound **1** by reduction of imine linkages with NaBH₄ in CH₃OH with good yield. Yield 81 %, mp ≥ 250°C. IR (KBr, cm⁻¹): ν = 3291, 2841, 2556, 1900, 1815, 1591, 1450, 1352, 1242, 1197, 1032, 968, 932, 873, 760 cm⁻¹; ¹H-NMR (300 MHz, CDCl₃): δ = 1.42-1.46 (d, 6H, 2-CH₃), 1.67-1.75 (bs, 2H, 2-OH), 2.72-2.80 (t, 4H, 2-CH₂-), 3.80-3.89 (q, 2H, 2=CH-), 6.74-7.17 (m, 8H, Ar-H), 11.38 (s, 2H, NH). ¹³C NMR (75 MHz, CDCl₃ = few drops of DMSO): δ = 21.1, 46.8, 58.9, 116.5, 119.0, 126.4, 127.9, 128.2, 156.9. LC-MS(M+H⁺) calcd for C₁₈H₂₅N₂O₂ = 301.19, found for C₁₈H₂₅N₂O₂ = 301.07. CHN Analysis; Calcd. C, 71.97; H, 8.05; N, 9.33; Found C, 71.82; H, 8.19; N, 9.37.

Cation recognition studies

The cation recognition studies were performed at ambient temperature (25°C), and the solution was repeatedly shaken before recording absorption and emission spectra to ensure uniformity. The cation binding ability of receptor **2** was studied by adding fixed amounts (0.5 equivalent) of metal salts (1 mM) to a standard solution of receptor **2** (0.1 mM, 2 ml) in CH₃CN by keeping the solvent ratio constant throughout the experiment. The binding study was explored by using fluorescence spectroscopy.

UV-visible and fluorescence spectral measurements

For UV-Vis absorption and fluorescence spectroscopy, the metal ion Na⁺, K⁺, Mg²⁺, Al³⁺, Cs⁺, Ba²⁺, Ca²⁺, Sr²⁺, Fe³⁺, Co²⁺, Ni²⁺, Cu²⁺, Zn²⁺, Cd²⁺, Hg²⁺, Pb²⁺, Th⁴⁺, Ag⁺, and Bi³⁺ were added as their nitrates, Cr³⁺, Mn²⁺ were added as their chlorides, while U⁶⁺ was added as its sulphate. The solutions of metal salts (1 mM) were prepared in CH₃CN containing 1% H₂O for analysis with receptor **2**. The solution of receptor **2** (0.1 mM) was freshly prepared in CH₃CN containing 1% H₂O. This solvent ratio was kept constant throughout the experiment. The excitation was carried out at 278 nm for receptor **2** with 5 nm emission slit widths in fluorometer. For absorbance and fluorescence measurements 1 cm width and 3.5 cm height quartz cells were used.

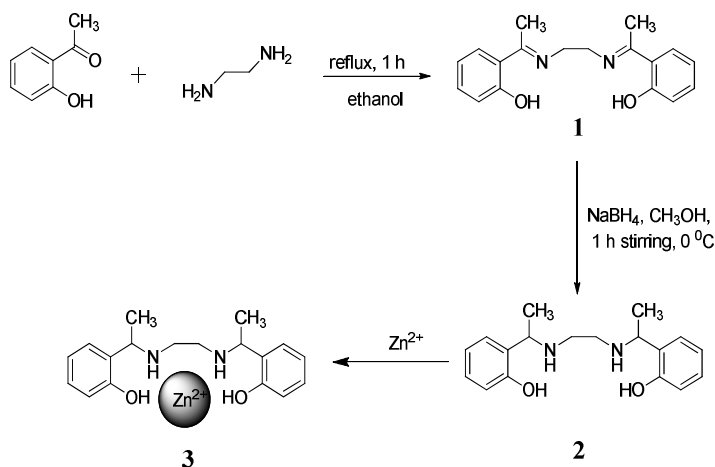
In vitro Cell imaging

Human cervical cancer cell HeLa was procured from National Centre for Cell Science, Pune, India and cultured in DMEM medium supplemented with 10% FBS and 2% L-glutamine-Penicillin-Streptomycin and maintained at 37°C in a humidified CO₂ incubator. The cells were seeded in the 35 mm culture dish with seeding density of 30 x 10⁴ cells. After reaching 60% confluence, complete media was replaced with serum free media. Immediately cells were treated with receptor **2** (2 μM) and incubated for 2 h. After washing the dish, fresh media was added and Zn²⁺ (25 μM) were also supplemented to the media. Live imaging of the cells were taken under fluorescence inverted microscope (Leica DMI 6000B) using UV and green excitation filter under 20x objective.

Result and Discussion

2,2'-{ethane-1,2-diylbis[nitrile(1E)eth-1-yl-1-ylidene]} diphenol (Compound **1**) was synthesized by refluxing an ethanol solution of 2-hydroxyacetophenone and ethane-1,2-diamine (2:1 molar ratio) for one hour. The reaction mixture was cooled and yellow coloured crystals of compound **1** were separated out. The crystals were filtered off and recrystallized from ethanol to give bright yellow crystals. Compound **1** was obtained with good yield.²¹ Further, receptor **2** was synthesized through reduction of compound **1** with NaBH₄ (Scheme 1). The synthesized receptor **2**

was characterized by melting point, IR, ¹H-NMR, ¹³C-NMR, mass spectroscopy (Figure S1-4).²⁸ The thermal behaviour of receptor **2** and **3** were studied using Thermogravimetric analysis (TGA) and Differential scanning calorimetry (DSC). TGA data shows that the sharp endothermic peak for decomposition of 2,2'-((ethane-1,2-diylbis(azanediy))bis(ethane-1,1-diyl)diphenol (**2**) and the **3** was obtained at 246.89 and 122.68 °C respectively (Figure S5a-b).



Scheme-1: Synthesis route of receptor **2** and **3**

The small initial weight loss in case of **3** may be attributed to crystalline water molecule. DSC data depicted in Figure S6a-b revealed that the endothermic peak at 111.87 and 114.74 °C corresponds to melting points of receptor **2** and the **3**. The small peak obtained at 106.81 may be owing to crystalline water molecule.

We tested the binding ability of receptor **2** by mixing it with Na⁺, K⁺, Mg²⁺, Al³⁺, Cs⁺, Ba²⁺, Ca²⁺, Sr²⁺, Cr³⁺, Mn²⁺, Fe³⁺, Co²⁺, Ni²⁺, Cu²⁺, Zn²⁺, Cd²⁺, Hg²⁺, Pb²⁺, Th⁴⁺, Ag⁺, Bi³⁺, and U⁶⁺ metal ions in CH₃CN containing 1% H₂O. The receptor **2** exhibited fluorescence emission maxima at 300 and 341 nm upon excitation at 278 nm. The fluorescence was selectively and significantly enhancement in the presence of Zn²⁺ ion. There was no such distinct fluorescence turn on observed in emission outline of receptor **2** in the presence of other tested metal ions, which indicated the high selectivity of receptor **2** for Zn²⁺ ion (Figure 1a). The enhancement of fluorescence was attributed to occurrence of the strong complexation to form **3**, resulting in the internal charge transfer (ICT) between array of two phenolic moieties along with two amines and zinc ion.^{29,30} These four atoms constitute a tetrahedral pseudo cavity for selective binding with zinc ion. The effect of increasing concentration of Zn²⁺ ion on the emission intensity of receptor **2** is pictured in Figure S7a-b. With increase of Zn²⁺ concentration, the emission intensity increased drastically and reached saturation with 8-fold enhancement at 385 nm when 1 equiv. (200 μl) of Zn²⁺ was added. From titration data, the dramatic change in the two emission maxima of receptor **2** at 300 and 341 nm was observed. Addition of Zn²⁺ up to 10 μl shows enhancement in both the peaks with comparatively less enhancement assisting with a blue shifting for the peak at 341 nm to 326 nm (Δλ = 15 nm) (Figure S7a). With further addition of Zn²⁺ ion solution, the resurgence in

the fluorescence intensity of the emission peak shifted at 326 nm followed by the restoring to its original position at 341 nm (upon addition of 100 μ l Zn^{2+} ion solution), with decrease in the emission peak at 300 nm assisted with a small red shift ($\Delta\lambda = 7$ nm). The further proceeding of Zn^{2+} ion solution addition shows enhancement in the emission maximum at 341 nm and decrease in emission intensity of the shifted peak at 307 nm. This provided judicious pathway for chelation-enhanced fluorescence (CHEF) between the Zn^{2+} ion and receptor **2** (Figure S7b).³¹ Also the significant sensing of Zn^{2+} ion by receptor **2** may be attributed to the tetravalent pseudocavity within the synthesized key receptor.³²

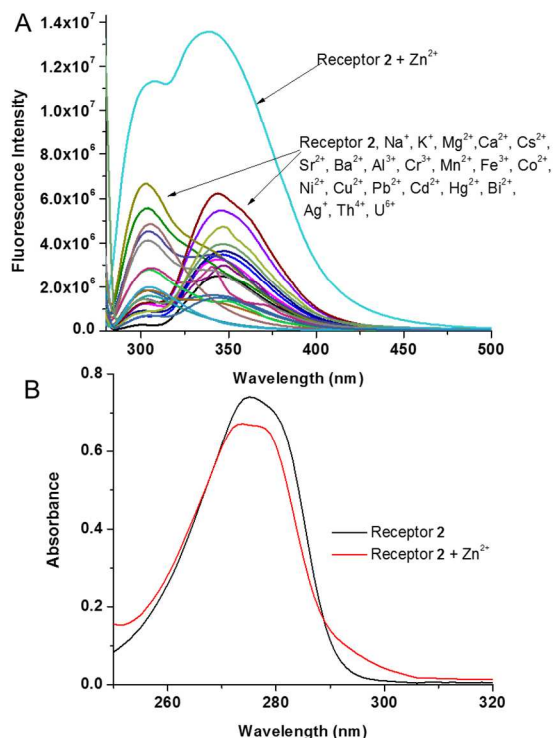


Figure 1. (A) Fluorescence emission spectra of receptor **2** (0.1 mM) in the presence of different cations (1 mM), at excitation $\lambda_{\text{ex}} = 278$ nm; (B) Absorbance spectra of receptor **2** (0.1 mM) with and without Zn^{2+} ion in CH_3CN containing 1% H_2O .

The reason of these dramatic changes in the fluorescence intensity of two emission maxima shown by receptor **2** was explained by the mole plot pictured in Figure S7c. It was revealed from the mole ratio plot the fluorescence enhancement up to 0.5 equivalent additions and further small decrease indicates formation of 2:1 complex between receptor **2** and Zn^{2+} and its subsequent dissociation. The further enhancement up to 1 equivalent addition (200 μ l) indicates 1:1 stoichiometry of **3**. The ongoing addition up to 2 equivalents indicates that the fluorescence intensity is barely changed, showing the stability of the 1:1 complex formed (Figure S7b-c).

Also the spectrofluorometric response of receptor **2** towards various metal ions was recorded and depicted in Figure S8 which shows that receptor **2** shows distinct fluorescence enhancement towards the Zn^{2+} ions compared to other metal ions. To study the

influence of other surveyed metal ions on Zn^{2+} ion binding with receptor **2**, we performed competitive experiments by mixing 2 equivalents of metal ions with 1 equivalent of Zn^{2+} ions (Figure S9). The observed fluorescence enhancement for mixtures of Zn^{2+} ion with surveyed metal ions was similar to that seen only for **3**. Thus no other metal ion appeared to interfere with the fluorescence intensity of the **3**. These results indicate that receptor **2** shows a significant sensitivity and selectivity towards Zn^{2+} ion over other studied competitive metal ions.

For practical reasons, the detection limit of receptor **2** for the analysis of Zn^{2+} ion was also an important parameter. Thus, based on the fluorescence titration measurement, detection limit of receptor **2** for Zn^{2+} ion was found to be 0.65 μM .³³ The low detection limit might fully meet the requirements in biosensing and comparable with literature reports as shown in Table S1. The stoichiometry of **3** complexation was studied using Job's continuous variation method.³⁴ The plot between $[\text{HG}] = \{(\Delta F/F_0)[\text{H}]\}$ and $X_i = [\text{H}]_v/([\text{H}]_v + [\text{G}]_v)$ has maxima at $X_i = 0.5$ which represents the 1:1 stoichiometry for **3** complexation which was also confirmed from the linear fitting of the normalized plot (Figure S10a-b). The stoichiometry of complexation was also confirmed by a Hill coefficient of 1.1446 obtained from a plot of $\text{Log} [(F - F_0)/(F_\infty - F)]$ vs $\text{Log}[\text{G}]$ (Figure S10c).³⁵ In addition, the formation of 1:1 complex between **2** and Zn^{2+} was further confirmed by the appearance of a peak at 369.5, assignable to $[(2.\text{Zn}^{2+}\text{-H}^+)(\text{H}_2\text{O})_{0.5}]$ in the LC-MS (Figure S11). The formation of such a Zn^{2+} complex can induce a π - π stacking interaction between two phenyl rings leading to a rather rigid structure with quite strong fluorescence properties, as compared to free receptor **2**.³⁶

With the purpose of comprehending the metal-binding properties of receptor **2**, the binding constant (K_d) value was calculated by Benesi-Hildebrand³⁷, Scatchard³⁸ and Connor's fitting³⁹ methodologies and value found from fluorescence data was $(1.00 \pm 0.1) \times 10^6 \text{ M}^{-1}$ which definitely make obvious the strong binding ability of **2** with Zn^{2+} (Figure S12a-c). The 1:1 binding ratio is also revealed from the linear fitting of the three methodologies. Further, to strengthen the coordination of Zn^{2+} ion complex, $^1\text{H-NMR}$ spectra of receptor **2** were recorded in the presence and absence of Zn^{2+} ion. It is observed that, the signals of $-\text{OH}$ proton at δ 1.67-1.75 get vanished upon addition of Zn^{2+} as shown in (Figure S13). These results clearly show that the $-\text{OH}$ protons of receptor **2** forms coordination with Zn^{2+} ion. Further, effect of pH has been studied on receptor **2** through varying the pH of the solution (Figure S14). It was observed change of pH did not produce any significant change in the fluorescence intensity of receptor **2** (Figure S15).

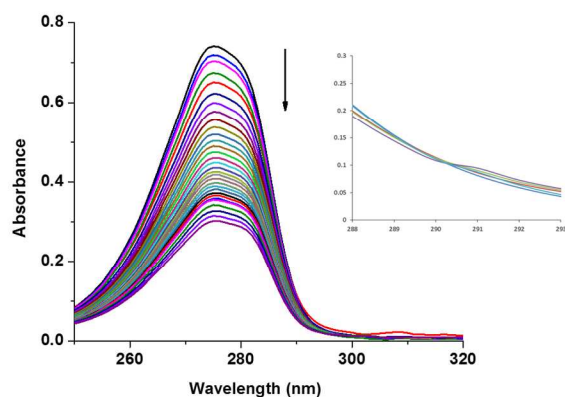


Figure 2: Change in absorbance spectra of receptor **2** upon continuous addition of Zn²⁺ ion in CH₃CN containing 1% H₂O; inset represent the isosbestic point of the titration.

The fluorescence intensity of receptor **2** was recorded at different temperature. With the increase of temperature, intensity was decreased and maximum intensity was observed at 25°C as shown in **Figure S16**. Further, response time has been calculated to optimize the complexation time and has response time of 41 sec (**Figure S16**).

The absorption spectrum of receptor **2** upon addition of Zn²⁺ ion is shown in **Figure 1b**. Receptor **2** exhibits peak maxima at 278 nm in CH₃CN. The addition of Zn²⁺ ion into receptor **2**, there had no change in receptor **2**. This is fact that the UV-Vis spectra of receptor **2** before and after the addition of 0.5 equivalent of Zn²⁺ showed moderate change, illustrated that it bounds with Zn²⁺ ion. Further, the titration was performed between Zn²⁺ and receptor **2** on UV-Visible spectrophotometer as shown in **Figure 2**. We also tried to grow the single crystal of Zn²⁺ complex of receptor **2**.

Unfortunately, we did not get crystals which are suitable for diffraction study. Therefore, to comprehend the electronic environment and changes in structure of receptor **2** upon complexation with Zn²⁺, a DFT calculation was performed using B3LYP/LANL2DZ basis set.⁴⁰⁻⁴² The optimized structure of receptor **2** has more or less similar geometry (**Figure 3a**). The two husks of receptor **2** having -OH groups are in opposite direction. Three electronegative atoms (O22, N26 and N25) arrange in particular way for encapsulation of analyte as shown in **Figure 3a**. On complexation with Zn²⁺ ion, the two -OH groups which are in opposite directions come against to each other (**Figure 3b**). It is noticed that a tetrahedral environment is constructed by oxygen and nitrogen atoms of -OH and -NH-groups for accommodation of Zn²⁺. For more clarification and better understanding, a comparison of geometrical parameters like bond length, bond angle and dihedral angle is made between **2** and **3** (**Table S2**). On carefully examine this table; it is observed that there is huge change in geometry of receptor **2** on complexation with Zn²⁺. A drastic change is observed in dihedral angles of C5-C4-C23-N25, C3-C4-C23-N25 and O22-C12-C11-C24 as shown in **Table S2**. It represents that atoms converge towards each other to form a pseudo cavity for Zn²⁺ ion. Further, all bond like N25-C29, C30-N26, C24-N26, C23-N25, C12-O22, C3-O21 showed increase in bond length upon addition of Zn²⁺ ion (**Table S2**). Similar, changes are observed in bond angles (**Table S2**).

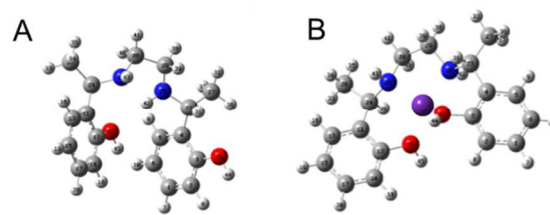


Figure 3. The DFT optimized structure of: (a) Receptor **2** and (b) 2.Zn²⁺ calculated at the B3LYP/LANL2DZ level. The red, blue, gray, and purple spheres refer to O, N, C, Zn²⁺ atoms respectively.

To test these probabilities and to determine the amount of colocalization of the two fluorophores, we incubated HeLa cells with 2 μM receptor **2**. Subsequent imaging with a dual-filter fluorescence microscope afforded the images shown in **Figure 4**. There was no fluorescence image observed when the cells were treated with receptor **2** alone, using UV and green excitation filter. There was faint cellular fluorescence observed when the cells were imaged under UV excitation filter in the presence of the receptor **2** and Zn²⁺ (**Figure 4D**).

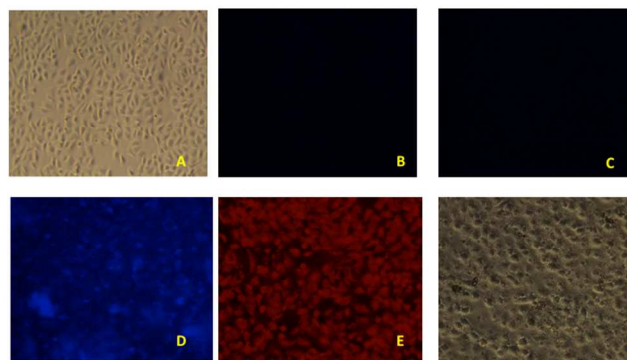


Figure 4 Imaging of HeLa cells treated with receptor **2** and Zn²⁺ (A) Phase contrast image of HeLa cells. (B) Fluorescence image of HeLa cells treated with receptor **2** (2 μM) (20X) and taken by UV excitation filter. (C) Fluorescence image of HeLa cells treated with receptor **2** (2 μM) (20X) and taken by green excitation filter. (D) Fluorescence photomicrograph of HeLa cells incubated with receptor **2** (2 μM) and Zn²⁺ (25 μM) (20X) taken by UV excitation filter. (E) Fluorescence photomicrograph of HeLa cells incubated with receptor **2** (2 μM) and Zn²⁺ (25 μM) (20X) taken by green excitation filter. (F) Phase contrast image of the cells treated with receptor **2** and Zn²⁺.

On the contrary, bright cellular image was observed when imaged under green excitation filter in the presence of the both receptor **2** and Zn²⁺ (**Figure 4E**). Qualitative assessment of the images specifies good intracellular overlap of the two fluorophores, an essential condition for the effectiveness of this sensing policy.

From the experimentation it is concluded that, a simple new fluorescence receptor **2** was prepared successfully with good yield. The receptor **2** has a high sensitivity and selectivity for Zn²⁺ ion. Receptor **2** shows a 8-fold fluorescence enhancement in the presence of 1 equivalent Zn²⁺ ion, and is not significantly affected by the presence of common physiologically and environmentally important earth- and transition metal ions. The high binding affinity of the synthesized key receptor and its changing stoichiometry towards the sensing of Zn²⁺ ion with its

increasing concentration is quite worth to mention here. Confocal microscopy experiments show that receptor **2** can be used for noticing changes in Zn²⁺ levels within living HeLa cells. Future arrangements will hub on improving the optical brightness and binding sympathy of this third-generation sensor as well as applying receptor **2** and related chemical instruments to sensor the cell biology of zinc.

Notes and references

^a School of Chemical Sciences, North Maharashtra University, Jalgaon-425001 (MS) India. kuwaras@gmail.com

^b School of Environmental and Earth Sciences, North Maharashtra University-Jalgaon-425001 (MS) India.

^c Department of Chemistry, Indian Institute of Chemistry, Ropar, Rupnagar (Punjab) India. nsingh@iitrpr.ac.in

^d Molecular Biology and Human Genetics Laboratory, Department of Zoology, The University of Burdwan, Burdwan, West Bengal, India.

1. L. B.Desmonts, D. N. Reinhoudt and M. C.Calama, Chem. Soc. Rev, 2007, **36**, 993.
2. R. Y. Tsien, in Fluorescent and Photochemical Probes of Dynamic Biochemical Signals inside Living Cells, ed. A. W. Czarnik, American Chemical Society, Washington, DC, 1993, 130.
3. A. P. de Silva, H. Q. Nimal Gunaratne, T. Gunnlaugsson, A. J. M. Huxley, C. P. McCoy, J. T. Rademacher and T. E. Rice, Chem. Rev, 1997, **97**, 1515.
4. Z. Xu, J. Yoon and D.R. Chem., Chem. Soc. Rev, 2010, **39** 1996.
5. Q. Zhao, F. Li and C. Huanga, Chem. Soc. Rev, 2010, **39**, 3007.
6. Y.D. Fernandez, A.P. Gramatges, V. Amendola, F. Foti, C. Mangano, P. Pallavicini, S. Patroni, Chem Commun, 2004, **14** 1650.
7. F. Kratz, B.K. Keppler, Metal complexes in cancer chemotherapy. VCH, Weinheim, 1993.
8. V. Amendola, L. Fabbrizzi, F. Forti, M. Licchelli, C. Mangano, P. Pallavicini, A. Poggi, D. Sacchi and A. Taglieti, Coord. Chem. Rev, 2006, **250**, 273.
9. R.R.Crichton, Biological Inorganic Chemistry: An Introduction, Elsevier, 2008.
10. E. Ochiai, Bioinorganic Chemistry: A Survey, Elsevier, 2008.
11. J.M. Berg, Y. Shi, Science, 1996, **271**, 1081.
12. J.H.Weiss, S.L. Sensi, J.Y. Koh, Trends Pharmacol. Sci, 2000, **21** 395.
13. R.M. Roat-Malone, Bioinorganic Chemistry: A Short Course, John Wiley & Sons, NJ, 2002.
14. S. W. Suh, J. W. Chen, M. Motamedi, B. Bell, K. Listiak, N. F. Pons, G. Danscher, C. J.Frederickson, Brain Res. 2000, **852**, 268.
15. D. W. Choi, J. Y. Koh, Annu. ReV. Neurosci, 1998, **21**, 347.
16. P. Roy, K. Dhara, M. Manassero, J. Ratha, and P. Banerjee, Inorganic Chemistry, 2007, **46**, 6405.
17. A. Takeda, BioMetals, 2001, **14**, 343; N. K. Wills, V. M. S. Ramanujam, N. Kalariya, J. R. Lewis and F. J. G. M. van Kuijk, Eye Res., 2008,878.; L. C. Costello and R. B. Franklin, Mol. Cancer, 2006, **5**, 17.
18. J. Mertens, F. Degryse, D.Springael, E. Smolders, Environ. Sci. Technol, 2007, **41**, 2992.
19. Y.Lv, M. Cao, J.Li and J. Wang, Sensors, 2013, **13**, 3131.
20. E.L. Que, D.W. Domaille, C.J. Chang, Chem. Rev, 2008, **108**, 1517.
21. B.Valeur, I.Leray, Coord. Chem. Rev, 2000, **205**, 3.
22. G.Q.Xie, Y.J.Shi, F.P.Hou, H.Y. Liu, L.Huang, P.X. Xi, F.J. Chen, Z.Z. Zeng, Eur. J. Inorg. Chem, 2012,**162**, 327.
23. G. Sivaraman, T. Anand and D. Chellappa, Analyst, 2012, **137**, 5881–5884.
24. J-A. Zhou, X-L. Tang, J. Cheng, Z-H. Ju, L-Z. Yang, W-S. Liu, C-Y. Chena and D-C. Baib, Dalton Trans., 2012, **41**, 10626–10632.
25. P. Li, X. Zhou, R. Huang, L. Yang, X. Tang, W. Dou, Q. Zhao and W. Liu, Dalton Trans., 2014, **43**, 706–713.
26. K. Kaur, M. Kaur, A. Kaur, J. Singh, N. Singh, S.K. Mittal and N. Kaur, Inorg. Chem. Front., 2014, **1**, 99–108.
27. Z. Dong, X. Le, P. Zhou, C. Dong and J. Ma, New J. Chem., 2014, DOI: 10.1039/c3nj01487h.
28. K. Tayade, J. Gallucci, H. Sharma, S. Attarde, R. Patil, N. Singh, A. Kuwar, Dalton Transactions, DOI: 10.1039/C3DT52690A.
29. Y. Maa, H. Chenb, F. Wanga, S. Kambama, Y. Wanga, C. Maoc and X. Chen, Dyes Pigm., 2014, **102**, 301-307.
30. X. Peng, Y. Xu, S. Sun, Y. Wua and J. Fan, Org. Biomol. Chem., 2007, **5**, 226-228.
31. F. Zapata, A. Caballero, A. Espinosa, A. T'arraga and P. Molina, Dalton Trans., 2010, **39**, 5429–5431.
32. H. Sharma, N. Kaur and N. Singh, Inorg. Chim. Acta., 2012, **391**, 83-87.
33. X.Y. Liu, D.R. Bai, S. Wang, Angew Chem, 2006,**118**, 5601.
34. P. Job, Ann Chim Appl, 1928, **9**, 113.
35. L. Tang, M. Cai, P. Zhou, J. Zhao, K. Zhong, S. Hou, and Y. Bian, RSC Adv, 2013, **3**, 16802.
36. M. Shellaiah, Y-H. Wu, A. Singh, M. V. R. Raju and H-C. Lin, J. Mater. Chem. A, 2013, **1**, 1310–1318.
37. H.A. Benesi, J.H. Hildebrand, J Am Chem Soc, 1949, **71**, 2703.
38. G. Scatchard, Ann NY Acad Sci, 1949, **51**, 660.
39. K.A. Connors, In Binding constants, The measurements of molecular complex stability. Wiley, New York, 1987.
40. C. Lee, W. Yang, R.G. Parr, Phys Rev, 1988, **B 37**, 785.
41. P.J. Hay, W.R. Wadt, J. Chem Phys, 1985, **82**, 270.
42. F. Wang, R. Nandhakumar, J.H. Moon, K.M.Kim, J.Y.Lee, J.Yoon, Inorg. Chem, 2011, **50**, 2240.

Graphical Abstract

